Journal of Alloys and Compounds 729 (2017) 338–343

Contents lists available at ScienceDirect

Journal of Alloys and Compounds

journal homepage: http://www.elsevier.com/locate/jalcom

Tailored perovskite $Li_{0.33}La_{0.56}TiO_3$ via an adipic acid-assisted solution process: A promising solid electrolyte for lithium batteries

Hyun Jun Choi [a], So Young Kim [a], Min Kyung Gong [a], Hari Vignesh [a], Vanchiappan Aravindan [b], Young Gi Lee [c], Yun-Sung Lee [a, *]

[a] Faculty of Applied Chemical Engineering, Chonnam National University, Gwang-ju, 500-757, South Korea
[b] Department of Chemistry, Indian Institute of Science Education and Research (IISER), Tirupati, 517507, India
[c] Power Control Device Research Team, Electronics and Telecommunications Research Institute, Daejeon, 305-700, South Korea

ARTICLE INFO

Article history:
Received 26 January 2017
Received in revised form
14 September 2017
Accepted 15 September 2017
Available online 18 September 2017

Keywords:
Solid electrolyte
Ionic conductivity
Phase transition
Perovskite
Sol-gel

ABSTRACT

We prepared and optimized the ionically conducting perovskite-type $Li_{0.33}La_{0.56}TiO_3$ by an adipic acid-assisted sol-gel process. A high ionic conductivity of 0.131 mS cm^{-1} was obtained at an ambient temperature by adjusting the synthesis temperature, holding time, and cooling process. A dramatic improvement in the $Li_{0.33}La_{0.56}TiO_3$ conductivity was noted in each step. Interestingly, a tetragonal-to-cubic structural transition was evident during the quenching process unlike in the conventional slow cooling process. An increase in the bottleneck site volume was observed that facilitated Li^+ ion migration for enhanced conductivity.

1. Introduction

Fabrication of high-energy Li batteries depends on the utilization cathodes with increased redox potential and high reversibility, as well as high capacity anodes. The limited thermodynamic stability window of conventional carbonate-based solutions strongly influences the electrochemical activity of the cathode and anode. Solvent molecule oxidation was observed above 4.5 V *vs.* Li, and a surface film of insoluble by-products was formed over the active material [1,2]. Similarly, a surface layer was formed by solvent molecule reduction below 1 V *vs.* Li. This surface layer increased the cell impedance and slowed the Li-ion diffusion kinetics. A carbonate-based solution allowed dendritic growth when metallic Li was employed as the anode. Leakage, flammability, and poor performance at an elevated temperature (>50 °C) were additional challenges of using liquid electrolytes [1–5]. Despite the high anode capacity (3862 mAh g^{-1}) of metallic Li, the current technology is based on "host-guest chemistry" with a graphite insertion anode. The graphite has a capacity profile nearly 10-times lower than that of Li but also experiences poor rate capability [6]. Dendrite formation on the graphitic surface occurs at high current operation. Metal oxide and phosphate-based insertion anodes along with conversion and alloy-type material reactive negative electrodes have been proposed as graphite alternatives but require sacrificing the energy density to overcome their inherent issues [6].

The use of solid electrolytes offers a promising solution to the challenges of liquid electrolytes and allows the exploration of high-voltage cathodes (>4.5 V *vs.* Li) with metallic Li as the anode [7–11]. Solid/dry polymer electrolytes and metal oxides (e.g. $Li_{3x}La_{2/3-x}TiO_3$, LLTO), sulfides (e.g. $Li_2S–P_2S_5$), and phosphates (e.g. $LiM_xZ_{2-x}(PO_4)_3$, M = Al, Z = Ti, Ge) belong to this category [1,12–16]. Polymer electrolytes provide advantages of leak proofing, flexibility, and versatility. However, the room-temperature conductivity has been too low for practical applications [16]. Attempts like filler incorporation in to polymer matrix, salt-in-polymer, has been reported but the conductivity is still insufficient for the room-temperature operation [17]. However, the mechanism of Li-ion transport (amorphous domains) in polymer electrolytes is entirely different.

LLTO is a promising solid electrolyte to explore compared to polymer electrolytes. The cation deficiency at the A site was favorable for monovalent cation conductivity through the

* Corresponding author.
E-mail addresses: aravind_van@yahoo.com (V. Aravindan), leeys@chonnam.ac.kr (Y.-S. Lee).

http://dx.doi.org/10.1016/j.jallcom.2017.09.160
0925-8388/

bottleneck formed by four adjacent BO_6 octahedra via ion hopping [18–22]. The ionic conductivity was dramatically increased when LLTO was paired with metallic Li compared to blocking electrodes like stainless steel. An increase in temperature increased the ionic transport. It was notable that the solid electrolytes exhibited 2- or 3-fold higher conductivity at an elevated temperature. Doping also increased the Li-ion diffusion by increasing the bottleneck volume. Fluoride ion substitution (F^- for O^{2-}) has also been attempted to improve the ionic conductivity [23]. The development of ionically conducting oxides could be efficiently used as solid electrolytes for emerging Li–O_2 and Li–S systems in addition to traditional Li-ion chemistry. Development of high-conducting solid electrodes is imperative to explore various Li-based secondary batteries. Synthetic methods of solid state, sol-gel synthesis [24], co-precipitation [25], spark plasma sintering, pulsed laser deposition, and microwave sintering have been adopted to synthesize LLTO. We explored an adipic acid-mediated Sol-gel technique to obtain highly conductive LLTO at ambient temperature by fine tuning the synthesis temperature, duration of holding time, and quenching or slow-cooling techniques with scalability in mind. The sol-gel technique is the common technique to obtain multi-component oxides with proper homogeneity and a smaller grain size. The sol-gel process can also assist in the formation of metastable phases with controllable composition, which is impossible by conventional synthetic processes. Further, we used adipic acid as a gelating agent to yield a homogeneous distribution of particles with a reduced grain boundary. Ambient temperature ionic conductivity and the influence on the structural properties were continuously monitored during this process. A dramatic increase in the room-temperature conductivity was observed and discussed in detail.

2. Experimental section

2.1. Synthesis

The starting materials of $Li(CH_3OO)\cdot H_2O$, $La(CH_3COO)_3\cdot 1.5H_2O$, TiO_2, and $C_6H_{10}O_4$ were received in high purity and used as such. The acetates were dissolved in distilled water at a stoichiometric ratio, and the TiO_2 particulates were dispersed within the solution through ultrasonication in a water bath. Adipic acid was dissolved separately and mixed into the solution. The resultant solution was continuously stirred at 180 °C on a hotplate. Water was evaporated, and the dry powder was kept under vacuum at 60 °C overnight with subsequent sintering at 600 °C over 10 h to decompose the acetate and di-carboxylate moieties. The resultant products were collected. A pellet was formed and fired between 1100 and 1200 °C for 5–24 h in air by adopting either the slow cooling or the quenching technique (Fig. 1).

2.2. Characterization

Powder X-ray diffraction (XRD) measurements were performed using a diffractometer (Rint 1000, Rigaku, Japan) with CuK_α radiation. Morphological studies of the LLTO were conducted with a field emission scanning electron microscope (FE-SEM, S4700, Hitachi, Japan) and a transmission electron microscope (TEM, Tecnai F20, Philips, Holland). Ionic conductivity measurements were performed using two stainless steel blocking electrodes in a conventional conductivity measurement setup. Before these measurements, a LLTO pellet (14 mm dia × 1 mm thick) was prepared and Pt was coated on both sides (~30 nm) to avoid interfacial issues. AC impedance analysis was conducted using 4284A Precision LCR Meter between 1 and 25 Hz with applied amplitude of 1 mV.

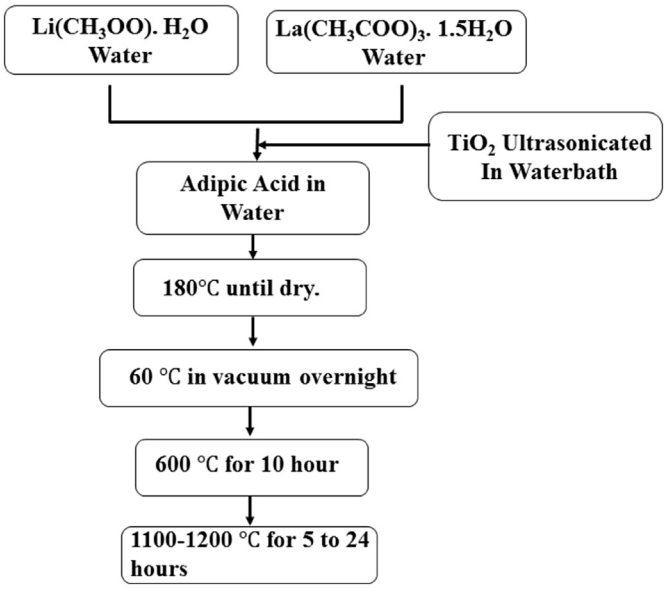

Fig. 1. Flowchart for the synthesis of $Li_{0.33}La_{0.56}TiO_3$ via adipic acid-assisted sol-gel synthesis.

3. Results and discussion

3.1. Temperature optimization

The temperature condition was optimized by firing the product between 1100 and 1200 °C at 20 °C intervals in air atmosphere for 5 h. The XRD patterns of the collected samples are given in Fig. 2a. The observed high-intensity reflections indicated the crystalline nature of the materials that corresponded to a tetragonal structure. The presence of TiO_2 was observed as a secondary phase up to 1160 °C with additional impurity peaks. Beyond this temperature, the primary phase decomposed and reacted with TiO_2. $La_2Ti_2O_5$ appeared as a new secondary phase that was evident in the XRD studies. These impurity peaks may have increased barriers of Li-ion diffusion that resulted in very low ionic conductivity. This result suggested that fine-tuning of the synthesis conditions were required to obtain a pure phase. Two additional samples were prepared at 1165 and 1170 °C with the same synthesis procedure. The corresponding images are given separately for proper understanding. A nearly pure phase without additional peaks was noted at 1165 °C. The secondary phase $La_2Ti_2O_5$ started to appear above 1170 °C. This result suggested that the temperature of 1165 °C was appropriate to obtain a single-phase material. Fig. 2c shows the FE-SEM image of LLTO prepared at 1165 °C. A weakly aggregated particulate morphology was evident with homogeneously distributed rectangular grains. The magnified image in Fig. 2d shows the well-defined grain boundaries. The microstructure was dense with a minimally scattered porous structure. At this very high temperature, porosity was scarcely distributed. The average grain size was less than 2 μm.

Increased ionic conductivity is imperative for solid electrolyte use in practical configurations. Pellets with a 14 mm diameter and 1 mm thickness were coated with Pt (~30 nm thick) and then sandwiched between two blocking electrodes for conductivity measurements under ambient temperature conditions (Fig. 3). High impedance on the order of kΩ was noted in all cases. LLTO resistance increased in the presence of TiO_2 to a greater extent than that in the presence of $La_2Ti_2O_5$. The LLTO prepared at 1165 °C had an ambient temperature conductivity of 7.8×10^{-8} S cm^{-1}. This

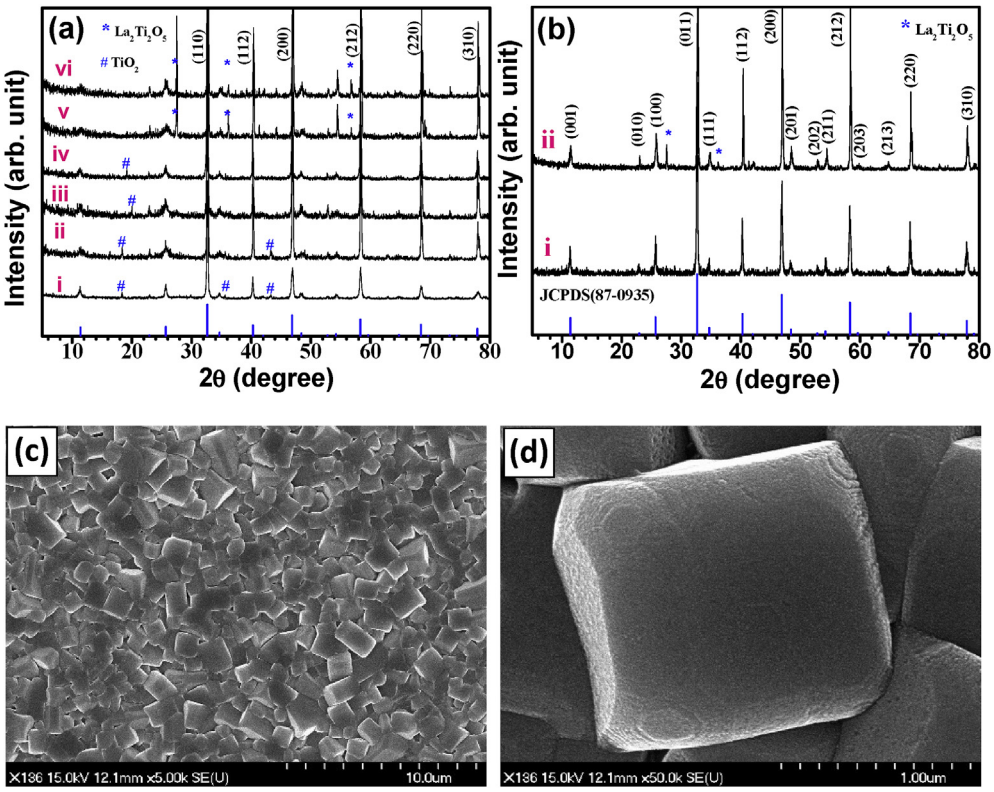

Fig. 2. (a) XRD patterns of $Li_{0.33}La_{0.56}TiO_3$ materials obtained at (i) 1100 °C, (ii) 1120 °C, (iii) 1140 °C, (iv) 1160 °C, (v) 1180 °C, and (vi) 1200 °C by sol-gel method, (b) XRD patterns of $Li_{0.33}La_{0.56}TiO_3$ materials obtained at (i) 1165 °C and (ii) 1170 °C, (c–d) FE-SEM pictures of $Li_{0.33}La_{0.56}TiO_3$ prepared at 1165 °C with different magnifications.

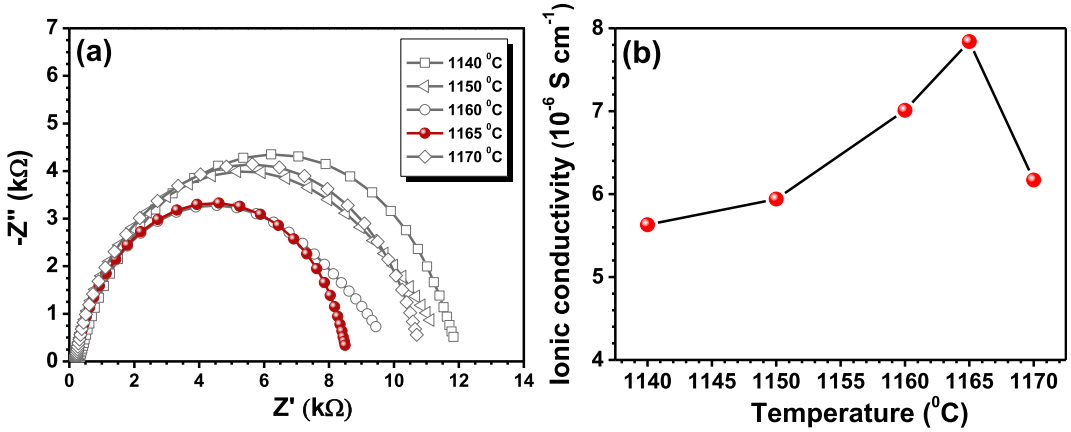

Fig. 3. (a) EIS curves of $Li_{0.33}La_{0.56}TiO_3$ materials calcined at various temperatures and (b) Plot of temperature *vs.* ionic conductivity.

conductivity did not meet the practical application requirement regardless of LIB, Li–O_2, or Li–S charge storage systems. Therefore, further optimization of the LLTO is desperately needed for reality.

3.2. Holding time optimization

Holding time was vital to the metal oxide crystallization and influenced the ionic conductivity of LLTO. The LTTO was prepared by varying the sample holding time from 5 to 24 h with a fixed final calcination temperature of 1165 °C in air. No traces of impurities were detected in the sample at this temperature. However, a notable deviation from the lattice parameter and cell volume was observed when the duration of the calcination process was altered as shown in Table 1 [22,24]. The *a* and *c* values, as well as cell volume, were increased as holding time increased. The bottleneck also where the Li^+ ion migration took place. Therefore, increased ionic conductivity was anticipated as holding time increased. All

Table 1
Lattice parameter values of LLTO prepared at different holding time.

Sintering duration	a(Å)	c(Å)	V(Å^3)
5 h	3.869(3)	7.740(6)	115.88(8)
10 h	3.870(4)	7.746(2)	116.03(6)
20 h	3.870(8)	7.747(2)	116.07(5)
24 h	3.872(8)	7.745(9)	116.17(7)

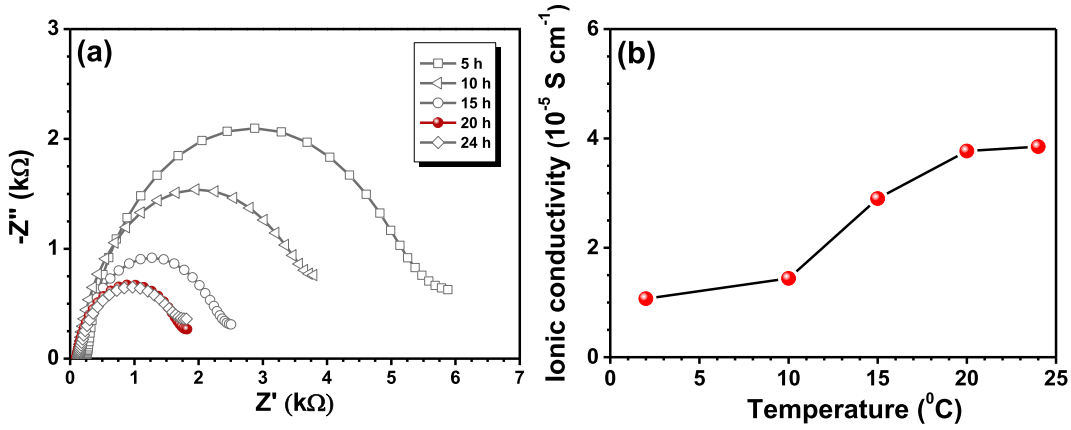

Fig. 4. (a) EIS curves of $Li_{0.33}La_{0.56}TiO_3$ materials calcined at 1165 °C with different holding time, (b) plot of ionic conductivity vs. holding time.

the samples were subjected to ionic conductivity measurements at ambient temperature conditions between a pair of blocking electrodes as shown in Fig. 4. A maximum conductivity of 3.85×10^{-5} S cm^{-1} was registered for a duration of 20 h, which was consistent with the variation in unit cell volume and deviation from the lattice parameter values. Alteration of holding duration enhanced the conducting profiles by three orders of magnitude. A negligible variation in the LLTO powder properties was noted in the sample treated for 24 h. No obvious differences between the conducting profiles were noted between the 20 and 24 h treatment durations. This result suggested that a holding time of 20 h at a temperature of 1165 °C was required to obtain a high-conducting LLTO.

3.3. Cooling condition

The cooling condition was also vital the conducting properties of solid, high ionically conducting metal oxides. The conventional

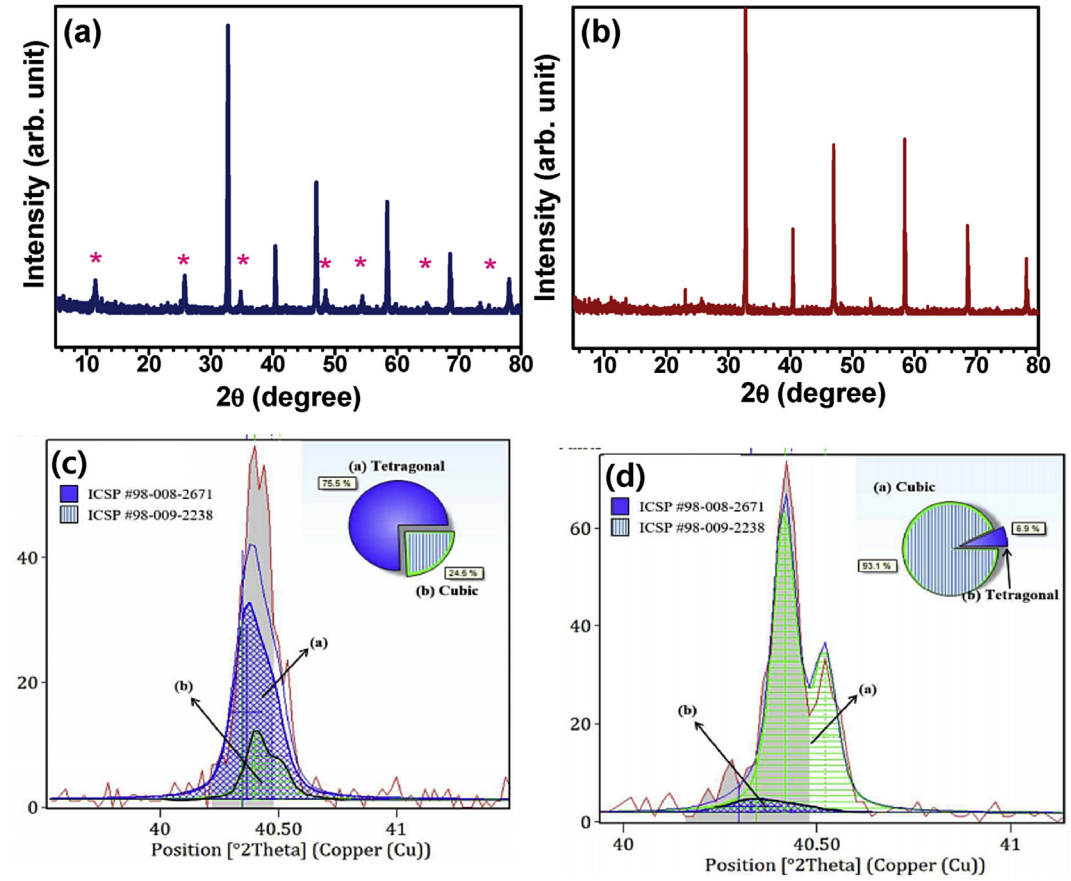

Fig. 5. XRD patterns of $Li_{0.33}La_{0.56}TiO_3$ obtained by (a) slow cooling, (b) quenching, (c) Deconvoluted XRD pattern of LLTO prepared by slow cooling, and (d) Deconvoluted XRD pattern of LLTO prepared by slow quenching.

Table 2
Comparison of the lattice parameter values corresponding to the cooling processes.

	Cubic		Tetragonal	
	a [Å]	V [Å]	a [Å]	V [Å]
	3.870	57.96	3.874	116.25
Slow cooling	3.868(6)	57.89	3.874	116.09
Quenching	3.873(7)	58.13	3.886(1)	116.89

cooling ramp affected the desired phase formation in certain compounds. Quenching by sudden cooling from a high temperature to ambient conditions allows materials to retain the desired structural properties [25] (Table T1). We explored the influence of this cooling step on the LLTO conducting profiles. The sample was fired at 1165 °C for 20 h and either the quenching or slow cooling procedure (10 °C min^{-1}) was adopted. The XRD patterns were recorded for each LLTO sample (Fig. 5). The superstructure peaks disappeared during quenching. The presence of superstructures indicated an uneven distribution of the La ions in A1 and A2 sites and corresponded to the tetragonal phase [23]. The absence of superstructure was associated with the formation of cubic phase due to the complete disordering of La ions. The secondary phase was estimated from the specific area analysis beneath the XRD reflections. The slow cooling sample was composed of 75.5% tetragonal phase, and the remainder was cubic phase. The quenching sample was 93.1% cubic phase, and the remaining 6.9% was tetragonal phase. The 0.12° shift towards a lower angle was noted for the quenching process compared to a 0.05° shift towards a higher angle for the slow cooling process. This deviation was associated with the respective growth and shrinkage of the unit cell volume compared to that of the reference. The corresponding deviations from the lattice parameter values and cell volumes are given in Table 2 [22,24]. The increased cell volume subsequently led to an increase in the bottleneck of facile Li^+ ion migration. This observation suggested that quenching efficiently yielded high-performance material irrespective of phase changes. Raman analysis (Fig. S1) and high-resolution transmission & selected area electron diffraction patterns (Fig. S2) were recorded to confirm the phase transformation. The Raman spectra of the quenched material were less active that those of the slow-cooled material, which was consistent with the theoretical literature predictions. The *Eg* Raman mode at around 120 cm^{-1} was diminished, which indicated the phase transition at a higher temperature.

The ionic conductivity studies were performed by placing the quenched or slow-cooled LLTO between two stainless steel blocking electrodes. The corresponding EIS traces are given in Fig. 4. The quenched LLTO exhibited an improved ambient temperature conductivity of 1.31×10^{-4} S cm^{-1} compared to previously reported values. The observed conductivity was one order higher in magnitude than the conventionally cooled LLTO (3.85×10^{-5} S cm^{-1}). The observed conductivity was about 17.5 times higher than the LLTO processed at 1165 °C for 5 h. This remarkable improvement was due to the optimized firing temperature and holding time combined with the quenching process and subsequent phase transformation from tetragonal to cubic. Phase formation has a demonstrated influence on ionic conductivity. Further studies to reduce the LLTO thickness (<1 mm) should be considered to achieve increased conductivity for practical applications without compromising the freestanding ability. A metallic Li battery could be constructed in an all solid-state configuration with LLTO as separator-cum-electrolyte and commercial cathodes such as $LiNi_{0.5}Mn_{1.5}O_4$. The potential use of the same LLTO in Li–S and Li–O_2 assemblies should also be prioritized.

4. Conclusion

We demonstrated the successful preparation of high ionic-conducting solid electrolytes by an adipic acid-assisted solution process. An ambient temperature conductivity of 0.13 mS cm^{-1} was obtained from optimized synthesis conditions at 1165 °C for 20 h with subsequent quenching. The conventional cooling process showed a conductivity lower by one order of magnitude. The optimization of the temperature conditions, holding duration, and cooling process improved the conductivity in a scalable manner. Studies to further improve the conductivity and suitability of LLTO as a solid electrolyte for rechargeable Li metal batteries are in progress.

Acknowledgments

We acknowledge financial support from the R&D Convergence Program of NST (National Research Council of Science and Technology) of the Republic of Korea. VA thank the financial support from the Science and Engineering Research Board, a statutory body of the Department of Science & Technology, Govt. of India through Ramanujan Fellowship (SB/S2/RJN-088/2016).

Appendix A. Supplementary data

Supplementary data related to this article can be found at http://dx.doi.org/10.1016/j.jallcom.2017.09.160.

References

[1] Y. Wang, W.D. Richards, S.P. Ong, L.J. Miara, J.C. Kim, Y. Mo, G. Ceder, Design principles for solid-state lithium superionic conductors, Nat. Mater. 14 (10) (2015) 1026–1031.
[2] N. Kamaya, K. Homma, Y. Yamakawa, M. Hirayama, R. Kanno, M. Yonemura, T. Kamiyama, Y. Kato, S. Hama, K. Kawamoto, A. Mitsui, A lithium superionic conductor, Nat. Mater. 10 (9) (2011) 682–686.
[3] Kang Xu, Nonaqueous liquid electrolytes for lithium-based rechargeable batteries, Chem. Rev. 104 (10) (2004) 4303–4418.
[4] V. Aravindan, J. Gnanaraj, S. Madhavi, H.K. Liu, Lithium-ion conducting electrolyte salts for lithium batteries, Chemistry 17 (51) (2011) 14326–14346.
[5] Renjie Chen, Wenjie Qu, Xing Guo, Li Li, Feng Wu, The pursuit of solid-state electrolytes for lithium batteries: from comprehensive insight to emerging horizons, Mater. Horiz. 3 (6) (2016) 487–516.
[6] Vanchiappan Aravindan, Yun-Sung Lee, Srinivasan Madhavi, Research progress on negative electrodes for practical Li-Ion batteries: beyond carbonaceous anodes, Adv. Energy Mater. 5 (13) (2015) 1402225.
[7] Yuki Kato, Satoshi Hori, Toshiya Saito, Kota Suzuki, Masaaki Hirayama, Akio Mitsui, Masao Yonemura, Hideki Iba, Ryoji Kanno, High-power all-solid-state batteries using sulfide superionic conductors, Nat. Energy 1 (4) (2016) 16030.
[8] J. Li, C. Ma, M. Chi, C. Liang, N.J. Dudney, Solid electrolyte: the key for high-voltage lithium batteries, Adv. Energy Mater. 5 (4) (2015) (n/a-n/a).
[9] J. Goodenough, Ceramic solid electrolytes, Solid State Ionics 94 (1–4) (1997) 17–25.
[10] J.B. Goodenough, P. Singh, Review—solid electrolytes in rechargeable electrochemical cells, J. Electrochem. Soc. 162 (14) (2015) A2387–A2392.
[11] John B. Goodenough, Youngsik Kim, Challenges for rechargeable Li batteries†, Chem. Mater. 22 (3) (2010) 587–603.
[12] Yoshikatsu Seino, Tsuyoshi Ota, Kazunori Takada, Akitoshi Hayashi, Masahiro Tatsumisago, A sulphide lithium super ion conductor is superior to liquid ion conductors for use in rechargeable batteries, Energy Environ. Sci. 7 (2) (2014) 627–631.
[13] V. Thangadurai, W. Weppner, Solid state lithium ion conductors: design considerations by thermodynamic approach, Ionics 8 (3–4) (2002) 281–292.
[14] Philippe Knauth, Inorganic solid Li ion conductors: an overview, Solid State Ionics 180 (14–16) (2009) 911–916.
[15] V. Thangadurai, S. Narayanan, D. Pinzaru, Garnet-type solid-state fast Li ion conductors for Li batteries: critical review, Chem. Soc. Rev. 43 (13) (2014) 4714–4727.
[16] Jeffrey W. Fergus, Ceramic and polymeric solid electrolytes for lithium-ion batteries, J. Power Sources 195 (15) (2010) 4554–4569.
[17] B. Scrosati, C.A. Vincent, Polymer electrolytes: the key to lithium polymer batteries, MRS Bull. 25 (03) (2000) 28–30.
[18] Myounggu Park, Xiangchun Zhang, Myoungdo Chung, Gregory B. Less, Ann Marie Sastry, A review of conduction phenomena in Li-ion batteries, J. Power

Sources 195 (24) (2010) 7904–7929.
[19] Yoshiyuki Inaguma, Chen Liquan, Mitsuru Itoh, Tetsurō Nakamura, Takashi Uchida, Hiromasa Ikuta, Masataka Wakihara, High ionic conductivity in lithium lanthanum titanate, Solid State Comm. 86 (10) (1993) 689–693.
[20] M. Itoh, Y. Inaguma, W.-H. Jung, L. Chen, T. Nakamura, High lithium ion conductivity in the perovskite-type compounds Ln12Li12-TiO3(Ln=La,Pr,Nd,Sm), Solid State Ionics 70 (1994) 203–207.
[21] M. Yashima, M. Itoh, Y. Inaguma, Y. Morii, Crystal structure and diffusion path in the fast lithium-ion conductor La0.62Li0.16TiO3, J. Am. Chem. Soc. 127 (10) (2005) 3491–3495.
[22] Qi Li, Juner Chen, Lei Fan, Xueqian Kong, Yingying Lu, Progress in electrolytes for rechargeable Li-based batteries and beyond, Green Energy Environ. 1 (1) (2016) 18–42.
[23] T. Okumura, T. Ina, Y. Orikasa, H. Arai, Y. Uchimoto, Z. Ogumi, Improvement of lithium ion conductivity for A-site disordered lithium lanthanum titanate perovskite oxides by fluoride ion substitution, J. Mater. Chem. 21 (27) (2011) 10061–10068.
[24] C. Cao, Z.-B. Li, X.-L. Wang, X.-B. Zhao, W.-Q. Han, Recent advances in inorganic solid electrolytes for lithium batteries, Frontiers Energy Res. 2 (2014) 25.
[25] Rohit Satish, Vanchiappan Aravindan, Wong Chui Ling, Srinivasan Madhavi, LiVPO4F: a new cathode for high-energy lithium ion capacitors, Chem. Select 1 (12) (2016) 3316–3322.